NUMERICAL ANALYSES OF NO_X FORMATION IN CYCLONE COMBUSTORS FED WITH AIR AND SAWDUST

Fábio Alfaia da Cunha
Departamento de Engenharia Mecânica, Centro Tecnológico, Universidade federal do Pará. Rua Augusto Corrêa nº 1, Guamá, Belém – PA – Brasil, CEP: 66075-110
alfaia@ufpa.br

Pedro Andrey Cavalcante Sampaio
Departamento de Engenharia Mecânica, Centro Tecnológico, Universidade federal do Pará. Rua Augusto Corrêa nº 1 , Guamá, Belém – PA – Brasil, CEP: 66075-110
asampaio@ufpa.br

Manoel Fernandes Martins Nogueira
Departamento de Engenharia Mecânica, Centro Tecnológico, Universidade federal do Pará. Rua Augusto Corrêa nº 1, Guamá, Belém – PA – Brasil, CEP: 66075-110
mfmn@ufpa.br

Gonçalo Rendeiro
Departamento de Engenharia Mecânica, Centro Tecnológico, Universidade federal do Pará. Rua Augusto Corrêa nº 1, Guamá, Belém – PA – Brasil, CEP: 66075-110
rendeiro@ufpa.br

Augusto Cesar de Mendonça Brasil
Departamento de Engenharia Mecânica, Centro Tecnológico, Universidade Federal do Pará. Rua Augusto Corrêa nº 1 , Guamá, Belém – PA – Brasil, CEP: 66075-110
ambrasil@ufpa.br

Abstract. *Reactive flow in cyclone combustors is complex due the coupling of a rotation turbulent flow with high temperature gradients. More complexity is added when the reactants flows are in two phases: air and sawdust. Optimization of the constructive and flow parameters can be achieved through the use mathematical modeling. This work presents the results of numerical calculation for NO_x and temperature radial profile in chosen section of a cyclone combustor burning sawdust in air. The mathematical modeling was made using the FLUENT computational code. The reactive turbulent flow was calculated using the combustion Presumed PDF/mixture fraction model with the k-ε RNG model. Temperature profiles and NO_x mol fraction distribution at critical section are for a cyclone combustor with diameter of 840 mm and height of 4000 mm.*

Keywords: *Cyclone Combustor; Fluent; Bioenergy; Sawdust combustion; NO_x production.*

1. Introduction

The woody biomass burners applied by sawmill industries in the Amazon Region are large and inefficient. It has as consequence that their by-products from manufacturing process burns slowly and their emissions have high concentration of pollutants as CO and hydrocarbon. The current solid combustion technology offers alternatives for this situation such as better furnace design or better type of combustor. A more efficient type of combustor is the cyclone furnace, because it is more compact, allows a complete combustion of the fuel, therefore, has a lower pollutant emission than the traditional burners. Cyclone combustor are applied to burn solid particle in suspension, and this solid particle can be anything containing carbons such as bark, sawdust, sander dust from plywood mills and even coke or petroleum residue (Ushima, 1998). The major constrain against the use of cyclone furnace is the fact that their emissions has high concentration of oxides of nitrogen (NO_x).

Advances in combustion knowledge showed that staged combustion reduces the formation of NO_x (Ragland 1998 and Syred et al 1974) and cyclones can take advantage of this technique. In order to achieve NO_x reduction, the combustion process must be understood and computational calculation has proof to a valuable tool. Initially, calculations were performed to identify what are the operation conditions that offer the minimal amount of NO_x at the cyclone outflow. These calculations were performed with CFD software considering a two-phase reagent flow and an Euler-Lagrange approximation (Bockelie et al 1998). Their results were in acceptable agreement with experimental results and allow the prediction the most suitable operational condition to reduce NO_x formation in cyclone furnaces but is not able to give an understanding of the formation process.

Once the process for NO_x was understood, it leads to combustion optimization and from there to the control of the pollutant emission. More recently, calculation with CFD-3D coupled with the commercial CFX-4 code were performed for a boiler with of 4 cyclone furnaces and having as a reagent inflow particles of coal in air (Berkstresser *et al* 2000),

having their equivalence ratio condition varying underfire to overfire. This work gave spatial resolution for the ignition region, the distribution of the species concentration and heat transfer flux in a cyclone combustion chamber.

Very recently, a 3-D calculation was performed for sawdust combustion in cyclone furnaces using the commercial code Fluent (Kops *et al* 2004) and the optimized operational conditions were obtained as well as the profiles for species concentrations and temperature. This calculation was able to predict the NO_x formation, but it did not consider the impact that changing the reagent equivalence ratio will cause on this formation. This work performed calculation for five different equivalence ratio of sawdust in air with the commercial code Fluent 6.0 and modeling the reagent flow in the combustion chamber with two techniques: the combustion mixture fraction/PDF and the turbulent k-□ RNG models.

2. Calculation Model

2.1 Model for turbulent flow: k-ε RNG

Reynolds equations describe the turbulent flow. The most common way to close the Reynolds equations is applying the Boussinesq hypothesis to related Reynolds stress to the mean velocity gradient, and this work also will do so. On the other hand, this work will not apply the regular k-□ model. Instead, one of its derivatives named k-ε RNG model (Orszag et al 1993) model was applied. This last model reduces scales on the Navier-Stoke equation using the renormalization group theory. The authors choose the derivative because this one is based on constants and functions theoretically deduced in opposite the empirical ones used on the standard k-ε model.

2.2 Model for combustion: Mixture fraction /PDF

The fraction mixture/PDF fraction is based on the solution for the transport equation for two conserved scalars named mixture fraction, *f*, and its variance, $\overline{f'^2}$. For a fuel/oxidizer system, the mixture fraction, f, is define as:

$$f = \frac{m_F}{m_F + m_{Ox}} \tag{1}$$

Where m is the mass, the subscrit Ox denotes oxidizer and the subscrit F fuel.

2.2.1 Conservation equations for the mixture fraction

Turbulent flows have its turbulent mass convection a few orders of magnitude bigger than the mass diffusion is reasonable to consider that the thermal diffusivity is equal to the molecular diffusion, Lewis number = 1 (Fluent 2003), therefore all the conservation equations are reduced to only one equation as a function of the mean mixture fraction $\bar{f}$.

$$\frac{\partial}{\partial t}\left(\rho\bar{f}\right) + \nabla\cdot\left(\rho\vec{v}\bar{f}\right) = \nabla\left(\frac{\mu_t}{\sigma_t}\nabla\bar{f}\right) + S_m \tag{2}$$

where $\vec{v}$ is the velocity, ρ is the air density, μ_t is the turbulent viscosity, σ_t is the turbulent Prandtl number. The source term S_m is due solely to transfer of mass into the gas phase from particles reacting. The mixture fraction/PDF model also demands that a solution for $\overline{f'^2}$ coming from the following conserve equation must be obtained.

$$\frac{\partial}{\partial t}\left(\rho\overline{f'^2}\right) + \nabla\cdot\left(\rho\vec{v}\overline{f'^2}\right) = \nabla\left(\frac{\mu_t}{\sigma_t}\nabla\overline{f'^2}\right) + C_g\mu_t\left(\nabla^2\bar{f}\right) - C_d\rho\frac{\varepsilon}{k}\overline{f'^2} \tag{3}$$

$f' = f - \bar{f}$, temporal fluctuation of f related to the its mean value. σ_t, C_g e C_d are constants with values 0.85, 2.86 e 2.0, respectively defined at Fluent´s manual 2003.

A scalar mean value due its variation during the turbulent fluctuations such as species concentration, density and temperature, they can be evaluated with the help of the probability density function, PDF. This function describe the time fluctuation of f due the effects of chemical reaction and turbulent flow.In this work the PDF is represented by the β-function that is given by following function:

$$p(f) = \frac{f^{\alpha-1}(1-f)^{\beta-1}}{\int f^{\alpha-1}(1-f)^{\beta-1}\,df} \tag{4}$$

Where: $\alpha = \bar{f}\left[\bar{f}\left(1-\bar{f}\right)/\overline{f'^2}-1\right]$ and $\beta = \left(1-\bar{f}\right)\left[\bar{f}\left(1-\bar{f}\right)/f'^2-1\right]$

2.3. Mechanisms for NO_x formation.

The mechanisms adopted for the production of NO_x are the Thermal mechanism and the Prompt mechanism(Turns 2004). The following species conservation equation for NO must be solved.

$$\frac{\partial}{\partial t}(\rho Y_{NO}) + \nabla.(\rho \vec{v} Y_{NO}) = \nabla.(\rho D \nabla Y_{NO}) + S_{NO} \tag{5}$$

Y_{NO} is the mass fraction of NO in the gas phase and S_{NO} is the source term.

Reactions (6)-(8) describe the thermal mechanism. Reaction (6), the initiation reaction, has high activation energy, meaning that this route only open when the reactants are at high temperature. During this calculation, the concentration of O and OH are assumed as in steady state and calculated through their partial equilibrium as recommended in the Fluent manual (Fluent 2003).

$$O + N_2 \Leftrightarrow N + NO \tag{6}$$

$$N + O_2 \Leftrightarrow O + NO \tag{7}$$

$$N + OH \Leftrightarrow H + NO \tag{8}$$

NO rate of reaction obtained from the above mechanism is

$$\frac{d[NO]}{dt} = k_5[O][N_2] + k_6[N][O_2] + k_7[N][OH] - k_{-5}[NO][N] - k_{-6}[NO][O] - k_{-7}[NO][H] \tag{9}$$

k_5, k_6 e k_7 are the rates coefficients for the forward reaction (6) - (8) and k_{-5}, k_{-6} e k_{-7} are rates coefficients for the reverse of the reactions (6) – (8).

The Prompt mechanism is important in fuel rich reactions and its reactions are expressed in equation from (10)–(14).

$$CH + N_2 \Leftrightarrow HCN + N \tag{10}$$

$$N + O_2 \Leftrightarrow NO + O \tag{11}$$

$$HCN + OH \Leftrightarrow CN + H_2O \tag{12}$$

$$CN + O_2 \Leftrightarrow NO + CO \tag{13}$$

$$CH_2 + N_2 \Leftrightarrow HCN + NH \tag{14}$$

2.4. Model for the flow of the solid phase

Fluent uses a Lagrange description for the solid phase flow. The changing in properties during its moving through the gas phase is represented for a set of ordinary differential equations representing the conservation equations of mass, momentun and energy. In this description, the initial properties and conditions of the solid phase are the input to start the calculation. The calculation results are the flow path, heat and mass transfer. The definition of how the solid phase is dispersed in the gas phase is determined through the stochastic tracking model. The equations of heating, volatilization and carbon oxidation are integrated through the calculated particle path. The calculation begins with the particle drying, than the its volatization and finally the particle oxidation what now is coal, being oxidation the process which last long (Ragland *et al*. 1998). The model adopted to describe the volatization is a first order reaction with an single kinetic rate.

$$-\frac{dm_p}{dt} = k\left[m_p - (1-f_{v,0})m_{p,0}\right] \tag{15}$$

where m_p is the temporal particle mass (kg), $f_{v,0}$ is the initial volatiles mass fraction in the particle, $m_{p,0}$ is the initial mass particle (kg), k is the rate constant (s^{-1}) following the Arrhenius definition for the rate constant: $k = A_1 e^{-(E/RT)}$. In this work choose A_1 and E as 7.0 E+7 s^{-1} and 1.2964 E+8 J/kgmol respectivally (Ragland 1998).

The surface reaction is a sink for the oxidant species and is a source of products species to the gas phase. In this work, the heterogeneous reactions on the particle surface are represented for the equation (16).

$$\frac{dm_p}{dt} = -A_p p_{ox} \frac{D_0 \Re}{D_0 + \Re} \tag{16}$$

where A_p is the superficial area of a particle (πd_p^2), p_{ox} is the oxidant partial pressure that involves a particle. The kinetic rate, $\Re = C_2 e^{-(E/RT_p)}$, incorporate the effects of chemical reaction on the internal surface of the char particle, residue of biomass volatilization and pore diffusion. The diffusion of the gaseous oxidant to the surface of the particle is given by

$$D_0 = C_1 \left[(T_p - T_\infty)/2\right]^{0,75} / d_p \cdot \tag{17}$$

3. The cyclone combustor

A cyclone combustor is a cylindrical chamber where air and solid particles follows a spiral flow path due the tangential entrance of the inflow in the combustion chamber. This kind of entrance causes a relative high speed between the particle and the air promoting high coefficients for heat and mass transfer and also high volumetric reaction rates, with values in the range of 4 to 8 MW/m^3 (Ushima, 1998). This kind of furnace, shown in the figure 1, is in its final stage of construction at the Mechanical Engineering Laboratory of the UFPA. It is 4,0 m tall with 0,84 m internal diameter and will be used to produce experimental results to validate the computational calculations.

(a)

(b)

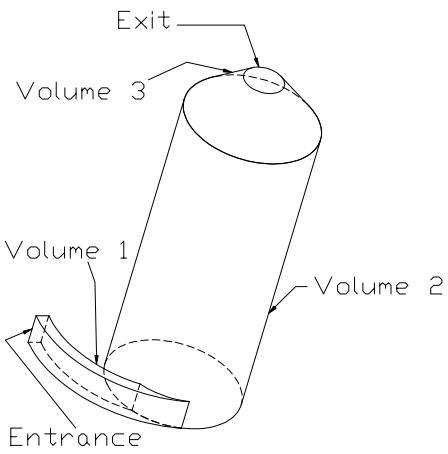

Figure 1. The cyclone furnace to obtain experimental data (a) and its geometry applied on calculations (b).

4. Geometry and mesh

All physical parameters needed were obtained from the cyclone furnace described in Figure 1(a) and the mesh needed for the Fluent perform the calculation was built with the software Gambit. As shown in Figure 1(b), the cyclone geometry was divided in three volumes, entrance, body and exit, to simplify the mesh construction. Hexaedron cells were used to create the mesh. FLUENT (2003) directions to built a mesh for combustion case are: low *EquiAngle Skew*: <0.9, moderate *aspect ratio* (<10), smooth changing on cell volume (<30%), the cell boundary should be as orthogonal as possible. The mesh built has 0,66 as maximum *Equi angle skew* and 7 as maximum *Aspect ratio*. The combustor mesh ended up with 105.000 cells.

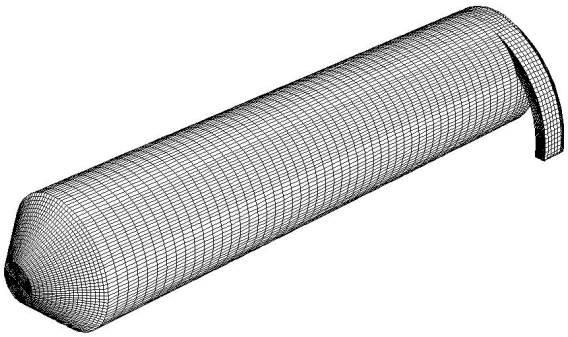

Figure 2. Combustor mesh.

5. CFD calculation

As described before, Fluent v. 6.0 code was applied to solve the governing equations for finite volumes from a system of non-structured mesh. As suggest (Fluent 2003) for flows with high swirl number, PRESTO methodology for interpolation was applies at pressure equation. The second-order upwind scheme was applied to the momentum equation, to the turbulent model, to the mixture fraction and to the mixture variance fraction. SIMPLE was the applied algorithm for coupling pressure and velocity. The model adopted for radiation heat exchanging was the discrete ordinate, the adopted particle emissivity was and the scattering factor equal 0,9 (FLUENT, 2003). Near the combustor wall, the solver uses wall functions to compute velocity, temperature and species concentration fields. This region goes orthogonally from the wall up to the half of the immediate adjacent cell.

Before the combustion calculation, input data must be processed through the PrePDF sub-routine. It is a pre-processor that request as input the list of working species together with their elementary composition, thermo-chemical properties, the fuel low heating value, specific heating and the inflow temperature. PrePDF uses this information to calculate mol fraction, enthalpy of formation, equilibrium concentrations and sensible enthalpy for all species at the inflow conditions. Outputs are look-up tables where mean values of mass fraction, density and temperature for all species are tabulated as function of mean mass fraction, variance and enthalpy.

6. Characteristics of biomass fuel

The characterization of used biomass was done at the Energy, Biomass and Environment Laboratory – EBMALab, at UFPA. Physical properties of woody biomass, mass basis, were obtained and are reported in the following table 1.

Table 1. Measured physical properties of woody biomass; mass basis.

Elemental analysis (%)		Physical properties (%)	
C	52,7	Volatiles	31,5
H	6,01	Fix Carbon	44
O	41,28	Ash Composition	0,99
N	-	Moisture Content	23,5
Cl	-	Higher Heating Value (MJ/kg)	19,77

Table 2 shows a list of adopted physical properties due the EBMALab is not able to make measurements and the respective source of such information.

Table 2. Adopted physical properties of woody biomass; mass basis.

Physical properties		Source
Density (kg/m^3)	500	Ragland (1991)
Specific heat (J/kg-K)	1760	Van Wylen (1993)
Thermal conductivity (W/m-K)	0,173	Ragland (1998)
Pyrolysis temperature (K)	473	Ushima (1998)

7. Boundary conditions

No-slip condition was adopted at furnace wall what was assumed to be adiabatic with emissivity as 0,7. Mixture fraction and variance was assumed to be zero at the sawdust-air inlet. The velocity profile for air at the entrance was as

turbulent flow with the turbulent length-scale of 0,00609 and turbulent intensity of 5%. The velocity flow profile was assumed to be uniform with the mean value of 7 m/s and temperature of 25ºC. It represents a mass flow rate of 0,1475 kg/s.

At the outlet, the turbulent intensity was assumed also 5%, a hydraulic diameter 0,25 m and its pressure profile evaluated through the following expression.

$$\frac{\partial p}{\partial r} = \frac{\rho v_\theta^2}{r} \tag{18}$$

where $p(r=0) = p_0, r$ *is* radial distance from the furnace central line, v_θ is the tangent component of the velocity and p_0 is the pressure at the central line and assumed to be the atmospheric pressure.

76.800 trajectories were adopted for the solid particle during the calculation and there was adopted that particles hitting the furnace walls return with 50% of its momentum to the gas phase flow. Rossin-Rammler-distribution function was used to represent the particle-diameter distribution with $d_{\min} = 20\mu m$, $d_{\max} = 400\mu m$, $\bar{d} = 184\mu m$, $n = 2{,}64$.

The sawdust mass flow rate was varied to obtain different equivalence ratio as defined at table 2.

Table 3. Equivalence ratio and mass flow rate adopted in this work.

Equivalence Ratio	0,75	1,25	1,5
Mass flow rate (kg/s)	0,0151	0,0252	0,0303

8. Strategies to obtain the convergence of the simulations.

Calculation began without the radiation model. After the calculation converge, the radiation model was turned on and executed again the simulation with the care to perform successively reduction on the under-relaxation factor to avoid divergence.

76.800 trajectories for the solid particles were choose because higher the number of trajectories betters the stability of the calculation (Fluent 2003). Indeed, high number of these trajectories improves the calculation stability.

The solver was set up to perform in double precision and the convergence criteria for each control volume was the summation of absolute residues for each parameter must be smaller than 10^{-4}. Exception for this rule was for energy and radiation residues. These obeyed the criteria that their residues must be smaller than 1.5×10^{-6}.

9. Results

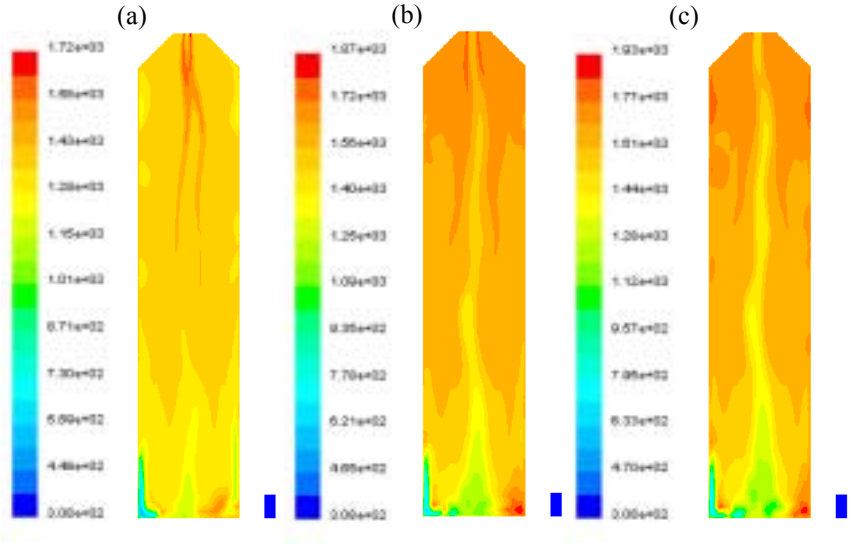

Figure 3. Longitudinal distribution for temperature at equivalence ratio of 0,75 (a), 1,25 (b) and 1,5 (c).

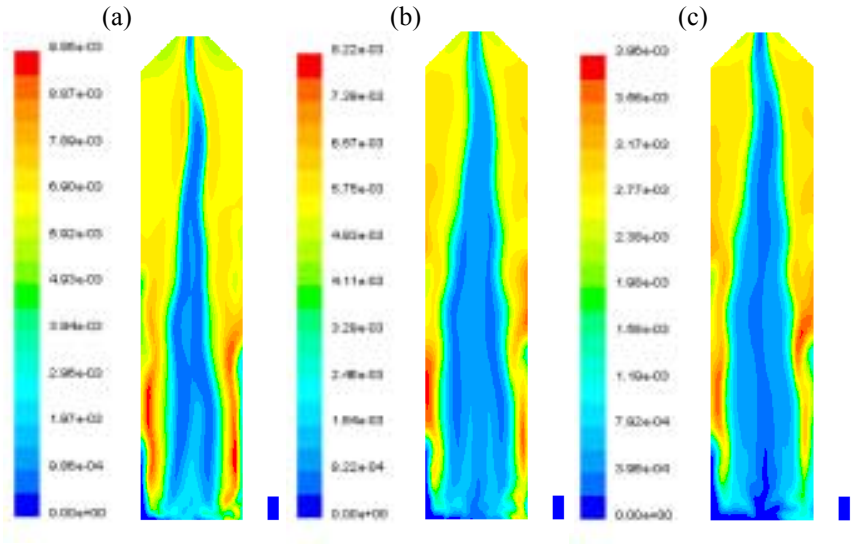

Figure 4. Longitudinal distribution of NO mole-fraction at equivalence ratio of 0.75 (a), 1.25 (b) and 1.5.(c)

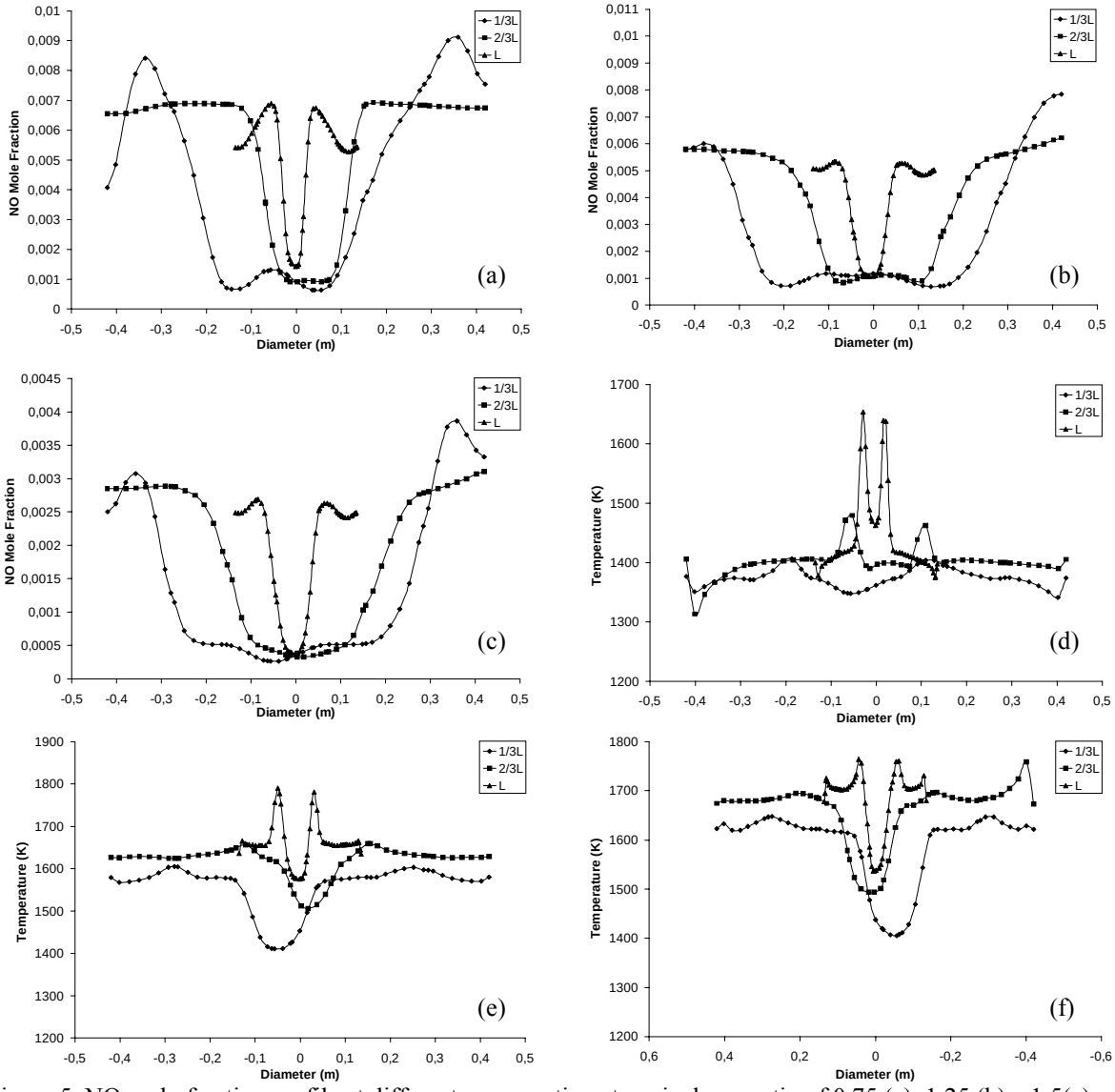

Figure 5. NO mole-fraction profile at different cross section at equivalence ratio of 0,75 (a), 1,25 (b) e 1,5(c). Temperature profile at equivalence ratio of 0,75 (d), 1,25 (e) e 1,5(f).

10. Summary and Conclusions

Figures 3a, 3b and 3c show temperature distribution in a longitudinal section of the furnace for three different equivalence ratio. All these figures show maximum temperature values for both, inlet and outlet regions. Furthermore, the temperature increases moving upward axially until arrive the maximum temperature near the exit. These results were obtained with the maximum air mass flow rate what caused the high temperature zone to be located near the exit. This is undesirable and must be considered as limiting conditions. It demands that simulations with lower flow rate must be done and it is actually under execution to aiming to improve the combustor efficiency.

Figures 4a, 4b and 4c show NO_x mole fraction distribution in a longitudinal section of the furnace for three different equivalence ratio. All figures indicate that the regions with high concentration of NO_x are located in regions near the furnace wall. Furthermore, the NO_x concentration rapidly increases from the inlet region to a maximum and then decreases gradually toward the combustor outlet. It is important to have in mind that the calculation was made for the highest flow rate allowed in the constructed furnace, therefore is the upper limit. Simulations with smaller flow rate are under execution and will be present in near future.

Figures 5a, 5b and 5c show profiles for radial temperature distribution in three different cross section height, 1/3, 2/3 and full height, for three different equivalent ratios. The output of figures 31, 3b, and 3c also are present here, which is the temperature increases following the longitudinal axis toward the exit achieving maximum near the outlet. As expected, the temperature are minimum near the combustor center, increasing outward in radial direction achieving a maximum and then decreasing up to meet the wall temperature.

Figures 5d, 5e and 5f show profiles for radial distribution of NO_x mole fraction in three different cross section, 1/3, 2/3 and full height, for three different equivalence ratio. At 1/3 of the burner height, region of lower temperature, the NO_x is minimum near the central and increasing with the radius achieving the maximum near the furnace wall. At the full height section, region with higher temperature, NO_x is minimum near the central axis, increasing with the radius up to the maximum and then decreasing up to the combustor wall.

11. References

Berkstresser, B., Walz, A., Michael, V. and Timothy, G., 2000, "Combustion Improvements While Controlling Emissions", Proceedings of 2000 International Joint Power Generation Conference Miami Beach, Florida.

Bockelie, M. J., Eddings, E. G., Adams, B. R., Valentine, J. R., Cremer, M. A., Smith, P. J., Davis, K. A. and Heap, M. P., 1998, "Computational Simulations of Industrial Furnaces. International Symposium on Computational Technologies For Fluid/Thermal/Chemical Systems with Industrial Applications", San Diego, California, USA.

Eaton, A.M., Smoot, L.D., Hill, S.C. and Eatough, C.N., 1999, "Components, formulations, solutions, evaluation, and application of comprehensive combustion models", Progress in Energy and Combustion Science", vol. 25, pp. 387–436.

FLUENT Inc., 2003, "FLUENT 6.1, User's Guide Volume", vol. 1-4, Lebanon, USA.

Fredriksson, Chistian, 1999, "Exploratory Experimental and Theoretical Studies of Cyclone Gasification of Wood Powder", Doctoral Thesis, Divison of Energy Engineering, Department of Mechanical Engineering, Lulea University of Technology.

Kops, S. M. B. and Malter, P. C., 2004, "Simulation and Modeling of Wood Dust Combustion in Cyclone Burners", Final Technical Report Prepared for U. S. Department of Energy.

Ragland, K. W., Aerts, D. J. and Baker, A. J., 1991, "Properties of Wood for Combustion Analysis", Bioresource Technology, vol. 37, pp. 161–168.

Ragland, K. W., and Borman, G. L., 1998, "Combustion Engineering", McGraw-Hill, USA.

Syred, N. And Beér, J. M., 1974, "Combustion in swirling flows: A review", Combustion and Flame, Vol. 23, pp. 143-201.

Turns, S. R., 2004, "An Introduction to Combustion", McGraw-Hill, USA..

Ushima, A. H., 2000, "Curso de Combustão Industrial", Brasil.

Van Wylen, G. J. & Sonntag, R. E., 1976, "Fundamentos da Termodinâmica Clássica"; Edgard Blucher.